Abstract

Specific Aims

The overall aim of this project is to develop new methods of determining the integrity of neurophysiological and hemodynamic processes in brain regions vulnerable to neurodegeneration.

A major area in functional magnetic resonance imaging (fMRI) research where insight is lacking is the relationship between neural activity and the blood oxygenation level dependent (BOLD) signal that constitutes the fMRI image. Though it is often assumed that the BOLD signal is a faithful reflection of neural activity it is becoming increasingly clear that normal aging and neurological diseases, such as neurodegeneration, can affect changes in neural activity as well as neurovascular coupling (NVC), both of which can lead to changes in the BOLD signal. This presents a major confound in the interpretation of fMRI images: to what extent do fMRI images reflect changes in neural activity and/or NVC? What is needed is an imaging method that disambiguates the neural and neurovascular components of the fMRI signal; and provides clinically useful measures sensitive to the integrity of NVC.

We propose to solve this problem using a method we have developed to non-invasively estimate the hemodynamic response to neural activity. Our approach uses simultaneously acquired electroencephalogram (EEG) and fMRI data, and is unique in being able to measure the hemodynamic response throughout the brain, and to do so in subjects at rest. The technique will allow, via deconvolution of the hemodynamic response, a more accurate estimation of the neural activity component of the fMRI signal; and provide a parameterized measure of NVC to assess the contribution of NVC changes to neurological diseases. This work is particularly timely and significant because of accumulating evidence implicating neurovascular dysfunction as an integral, and possibly causative, part of Alzheimer's disease. By separating measurement of neural activity and NVC our approach will provide a means to study changes in and interactions between these processes in healthy aging and disease, potentially leading to a greater understanding of these disease mechanisms; greater sensitivity and specificity in the development of biomarkers; and a more powerful way to track changes during disease development and drug intervention trials.

Specific Aim 1: Enhance detection of neural activation in the resting-state

Specific Aim 2: Estimate the neurally activated hemodynamic response throughout the cortex

Specific Aim 3: Validate use of simultaneously acquired EEG to estimate the neurally activated hemodynamic response throughout the brain in subjects at rest

We will compare the hemodynamic response obtained by our method with that obtained by event-related and breath-holding FMRI tasks.

Specific Aim 3: Characterize the neurophysiological and hemodynamic processes in cortical vascular border zones and cortical association areas in a population sample

Significance

At the basis of functional magnetic resonance imaging (FMRI) is a fundamental ambiguity - to what extent does variance in the fMRI images reflect changes in neural activity (as is commonly assumed) or changes in neurovascular coupling (NVC)? FMRI is increasingly being used to study clinical populations where there may be disease of the arterioles on which NVC depends, and where the blood oxygenation level dependent (BOLD) signal is known to be generated. We propose a method to disentangle these components, and in doing so simultaneously provide a major contribution to the scientific field of functional neuroimaging, and the clinical field of small vessel cerebrovascular disease.

Disambiguation of the Blood Oxygenation Level Dependent Signal

FMRI is the most widely used non-invasive method for imaging the functioning brain, with an exponential rise in publications reaching in excess of 350,000 (pubmed.gov as at Feb 2014). Yet the results from this body of research are often confounded by a fundamental ambiguity arising from the indirect nature of FMRI measurement: FMRI measures the state of blood oxygenation, which changes in response to neural activation. This project will develop a method to generate separate estimates of the neural and NVC components of the FMRI BOLD signal (hereafter called the FMRI signal). We aim to generate a more faithful estimate of the neural signal without the variance imposed by NVC factors, and provide an analysis of NVC per se, i.e. unconfounded by neural processes in disease. Importantly, this method will be able to do this non-invasively, throughout the cerebral cortex, and in subjects at rest. This is significant because it is becoming increasingly clear that NVC varies as a function of many factors including cortical region (Conner et al 2011, Handwerker et al 2004, D'Esposito et al 2003), aging (Kannurpatti et al 2010), disease (Lecrux & Hamel 2011, Hillary & Biswal 2007, D'Esposito et al 2003), ingested substances, and genetics (Handwerker et al 2012). Disambiguating the FMRI signal will first, provide an estimate of the neural signal with less variance induced by these factors, and second, provide a measurement of NVC potentially more sensitive to disease processes.

Estimation of the Hemodynamic Response in subjects at Rest and Throughout the Cortex

Our method non-invasively quantifies NVC parameters by estimating the hemodynamic response (HR) to neural activity using simultaneously acquired electroencephalogram (EEG) and FMRI data, and is unique in being able to estimate the HR in subjects at rest. This is significant because being able to use brain activity in subjects at rest means that the HR can be simultaneously estimated throughout the entire cortex. This, for the first time, makes it feasible to generate cortical maps of the integrity of the NVC system, which will make it an invaluable clinical tool for the assessment of brain health. Measuring the hemodynamic response in higher-association areas is important because these regions of cortex are preferentially targeted by some neurological diseases, including Alzheimer's disease.

Small Vessel Disease is a Good Model System for Studying Neurovascular Coupling

Small vessel cerebrovascular diseases (svCVD), including arteriolosclerosis and cerebral amyloid angiopathy, inflict a far greater number of microinfarcts than can be detected by current brain imaging methods (Smith et al 2012). svCVD is widely accepted to potentiate Alzheimer's disease, and both pathological components are the rule in autopsy studies of population-based samples (Montine et al 2012). Recent evidence suggests that svCVD plays an integral and possibly causative role in neurodegeneration through the impaired delivery of oxygen, glucose, nutrients, and clearance of neurotoxic molecules (Zlokovic 2011, Girouard & Iadecola 2006, Iadecola 2004). By measuring the HR throughout the cortex our method could potentially provide a non-invasive means to detect and monitor these neurovascular changes in svCVD. This is significant because the ability to monitor NVC changes in these diseases would be a major step toward understanding the interaction between svCVD and neurodegeneration; and would provide a more powerful way to track changes during disease development and drug intervention trials.

Innovation

Estimating the Neurally Activated Hemodynamic Response in Subjects at Rest

We demonstrate a non-invasive method that, for the first time, that the neurally activated hemodynamic response (HR) can be estimated in the brain of subjects at rest.

Although non-invasive methods exist to estimate the HR in the brain, these methods have limitations that render them of little clinical utility. Event-related fMRI (ER-FMRI) studies estimate the HR either by averaging the BOLD response to repeated stimuli or behavioral events spaced at long (~15 to 20 seconds) intervals (Handwerker et al 2004), or by deconvolving the BOLD response using the stimulus or response sequence (Miezin et al 2000). These methods activate only specific areas of the brain depending on the stimulus/response used, necessitating the need for repetition with different stimuli/responses to obtain greater brain coverage. This, of course, would take an exorbitant amount of time. Further, at some regions of the brain, such as higher-order association cortex, it is difficult to elicit a BOLD response to a stimulus. Indeed areas of the default mode network (DMN) show a decrease in the BOLD signal following a stimulus. TFD overcomes these limitations by estimating the HR without requiring a stimulus or response. Further, the HR can be estimated throughout the cortex, including higher-order association areas. This is important because higher-order association area dysfunction is a key feature of AD and other neurological diseases.

Estimating the HR in the resting state

ER-FMRI requires subjects to actively attend to stimuli and provide timely responses. This is undesirable in some clinical populations, such as mild cognitive impairment or dementia, where subjects might be less able to understand or remember to follow instructions. TFD overcomes these limitations by estimating the HR in subjects while they are at rest.

Detecting neural activation in the resting state

The TFD method uses a novel approach to detect neural activation in the resting state. At the same time a stimulus/response event triggers a HR in the BOLD signal, the EEG signal shows characteristic event-related synchronization (ERS) and event-related desynchronization (ERD) in different frequency bands (Boord; Pfurtscheller). Further, these frequency band changes occur in a fixed order. For example, it has been shown in the visual, motor, and auditory cortices that alpha power decreases (ERD) prior to and during a stimulus, whereas gamma power increases (ERS) after presentation of a stimulus (ref). This information can be captured in a time-frequency plot, or spectrogram, as shown in the primary visual cortex (EEG electrode Oz) from our preliminary data in Figure 2. We hypothesize that similar, though not necessarily identical, dynamics occur in activated cortex during the resting state. This is based, in part, on the observed functions of the different EEG rhythms. For example, in the sensorimotor cortex there is considerable evidence that alpha band frequencies have an inhibitory role, acting like an idling rhythm that it desynchronized by action, motor imagery, or action observation (Boord; Pfurtscheller). Further evidence supports a similar inhibitory role for alpha band activity in other areas of the cortex, including visual and auditory cortex (ref). Given that the role of activity in the alpha (and other) frequency bands is similar for different tasks and in different areas of cortex, we hypothesize that EEG frequency band activity will show similar behavior in the resting state. The TCD method, however, does not rely on the EEG dynamics being the same in event and resting states. Rather, it uses a novel signal processing technique to identify neural activation based on the consistency of neural dynamics in the resting state.

Approach

Preliminary Data: Estimating the Hemodynamic Response Function in the Resting-State

There are no reports of estimating the neurally activated hemodynamic response function (HRF) in humans in the resting-state (where no stimulus or response is performed). Here, the HRF refers to the impulse response of the NVC system, i.e. the shape of the transient FMRI signal that arises in response to a rapid burst of neural activity. We have successfully adapted an invasive method of HRF estimation recently demonstrated in anesthetized rats (Bruyns-Haylett et al 2013; BH-method). The BH-method detects negative peaks (current sinks) in local field potentials (LFP) from subdural electrodes implanted in layer four of the rat somatosensory cortex. The authors used these peaks as surrogate stimulus/response event markers, and demonstrated that averaging epochs of BOLD activity aligned to these peaks produced a HRF similar to that obtained using whisker stimulation (Bruyns-Haylett et al 2013).

Electroencephalography (EEG) has a much lower signal-to-noise ratio than LPF recorded subdurally, especially when the EEG is collected simultaneously with FMRI. We collected 10 minutes of simultaneous EEG-FMRI data in a subject at rest, and 20 minutes of data while the subject performed a visual stimulus/response task. The task involved the subject pressing buttons in both hands using their

thumb in response to a flashing checkerboard presented at 20-second intervals. Simultaneous EEG-FMRI was recorded using a Brain Products 64-channel BrainAmp MR in-magnet EEG amplifier, and a BrainCap MR EEG electrode cap. We successfully removed the MRI gradient and ballistocardiographic artifacts using the FMRIB plug-in for EEGLAB, provided by the University of Oxford Centre for Functional MRI of the Brain (FMRIB) (Niazy et al 2005; Iannetti et al 2005). We found the proprietary Brain Products software (BrainVision Analyzer 2) was unable to remove the MR artifacts in their entirety.

Figure 1A shows EEG collected from the visual cortex while our subject was at rest with eyes open and fixated. The EEG was recorded over the visual cortex from electrode site Oz using a Laplacian reference (average of sites O1, O2, POz) to provide an estimate of current density flowing out of the scalp. The BH-method looks for 'activation events' indicated as negative peaks within contiguous time-windows, exceeding a threshold of two standard deviations (S.D.) beyond the mean of the EEG signal. Figure 1A shows two such peaks as red circles in an approximately seven-second segment of EEG. The BH-method selects the largest of these peaks – the right red circle in Figure 1A in this example. A 20-second epoch is then obtained from the BOLD signal, originating at the time of the largest EEG peak – shown as the red square in Figure 1C. We repeated this process in 20-second contiguous time-windows comprising the 10-minute resting-state data, and then averaged all the 20-second epochs (30 in total) to estimate the HRF.

The resting-state HRF (R-HRF) is shown as a green line in Figure 2 for the left motor cortex (EEG electrode C3, Laplacian referenced), and in Figure 3 for the visual cortex. The black curve in Figure 2 and Figure 3 represents the event-averaged HRF (E-HRF) for the movement (button press) and visual stimuli (flashing checkerboard) respectively. The zero time-point represents the estimated time of cortical activation. For the resting-state this was defined by the location of the maximal negative peaks detected by the BH-method. For the visual and motor task the time of cortical activation was estimated as the maximal negative peak within a short time window following the visual stimulus: 100 to 200ms for the visual cortex (to detect the known N1 component in the visual evoked potential) or 100 to 1000ms for the motor cortex (to account for reaction time and detect the N1 or N2 component in the movement-related potential; Riehle et al 2013). It can be seen that the main (positive) HRF peak is essentially identical for movement and resting-state in the motor cortex. Both motor and visual R-HRF show no post-stimulus undershoot. The origin of the undershoot remains unclear (van Zijl et al 2012), however there is strong evidence suggesting it is modulated by post-stimulus activity (Mullinger et al 2013). The absence of undershoot, observed here in R-HRF for both visual and motor cortices, may indicate differences in cortical processing, for stimuli or rest, following initial cortical activation.

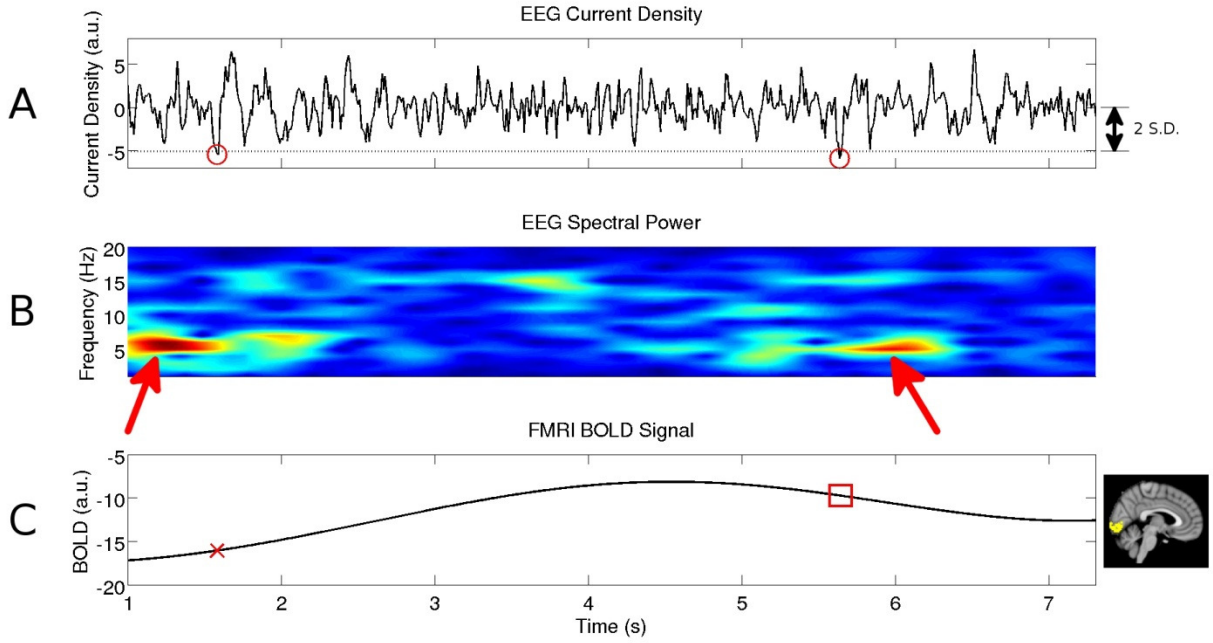

Figure 1 Estimating the hemodynamic response function in the resting-state. (A) Resting-state EEG signal overlying the visual cortex (electrode Oz). Red circles surround peaks exceeding a threshold of 2 standard deviations from the mean, and may indicate activation in visual cortex. The BH-method chooses the peak in the right red circle because it exceeds the threshold by a greater amount (Bruyns-Haylett et al 2013). (B) Time-frequency plot of the EEG time-series shown in (A), showing the frequency content at each time point. Red arrows point to two moments of high power in the 5-6 Hz band. The first moment of high power (left arrow) precedes the peak in (A) (left red circle). The second moment of high power (right arrow) follows the peak in (A) (right red circle). (C) Resting-state BOLD signal from visual cortex occurring simultaneously with EEG in (A). BOLD signal is averaged from region indicated in yellow on the brain image at right. The red square indicates the moment of neural activation estimated by the BH-method, which selects the largest peak in an interval. The red cross indicates a more likely moment of neural activation as it is preceded by high 5-6 Hz power, which is more typical of activation found in event-averaged and resting-state peak-averaged time-frequency plots (see Figure 4).

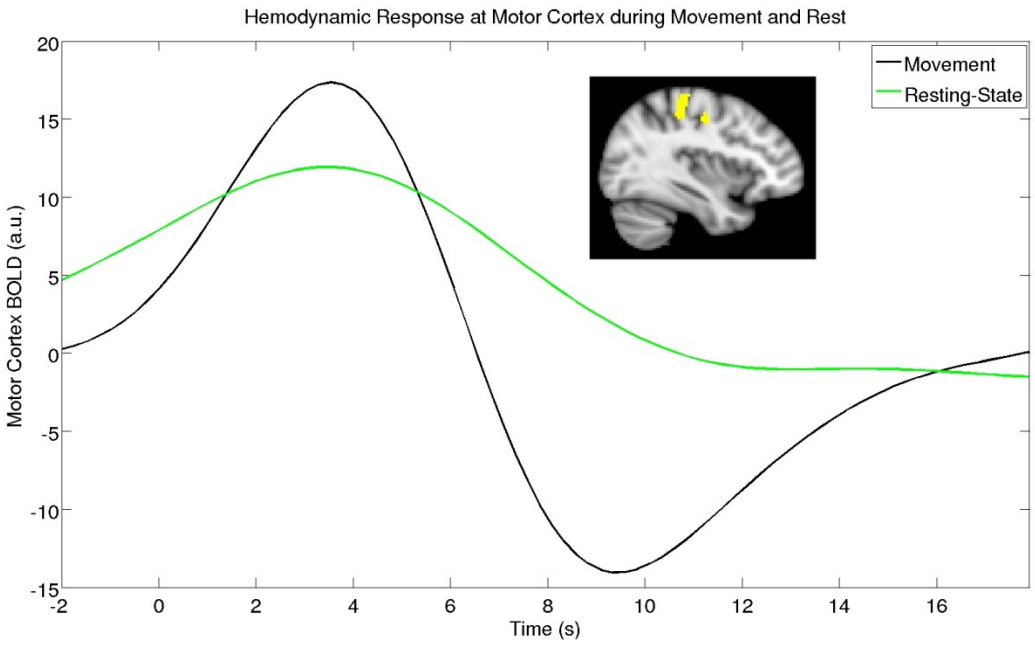

Figure 2 Motor cortex hemodynamic response function (HRF) during movement (black) and at rest (green). Each HRF is derived from the FMRI signal averaged over voxels in the left motor cortex thumb area, indicated by the yellow area superimposed on the brain image. The movement HRF (black) is an average of responses to button presses. The resting-state HRF (green) is an average of responses to significant negative peaks in the resting-state EEG.

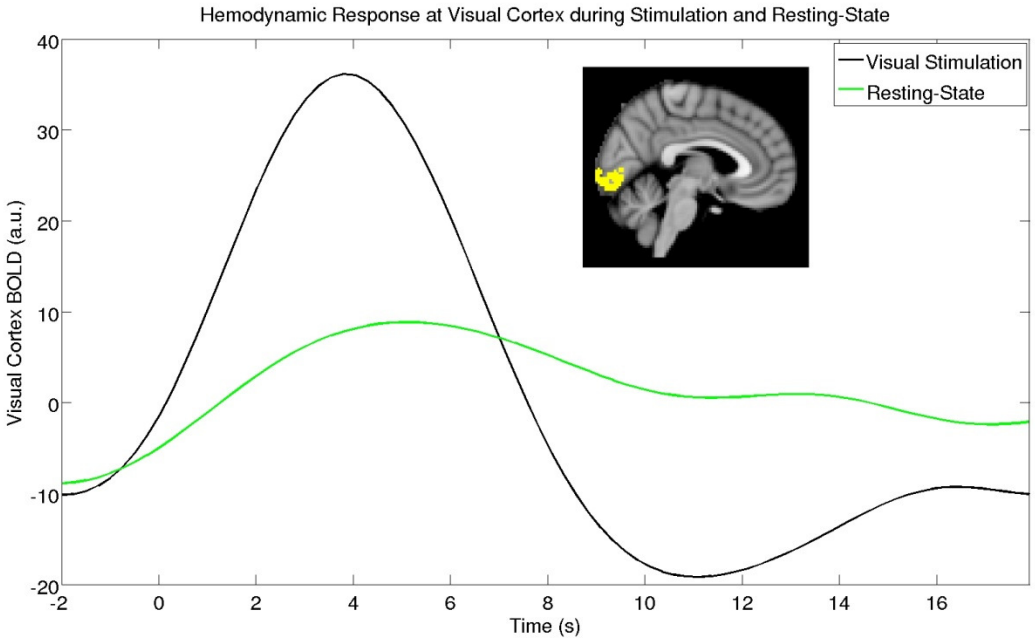

Figure 3 Visual cortex hemodynamic response function (HRF) during visual stimulation (black) and at rest (green). Each HRF is derived from the FMRI signal averaged over voxels in the primary visual cortex, indicated by the yellow area superimposed on the brain image. The visual stimulation HRF (black) is an average of responses to a flashing checkerboard pattern. The resting-state HRF (green) is an average of responses to significant negative peaks in the resting-state EEG.

Specific Aim 1: Enhancing Detection of Neural Activation in the Resting-State

A pitfall of the simple peak detection approach used by the BH-method is its susceptibility to artifacts, such as electrode pops: sudden electrode-scalp potential changes due to movement or dried electrode paste. Large false peaks could also come from head movements in the MRI magnet, which can induce transient currents in the EEG cap wires. While steps can be taken to minimize these artifacts or remove sections of EEG contaminated by these artifacts, there is still the possibility that artifacts could go undetected and lead to distortion in the HRF estimate through selection of false peaks in place of peaks marking neural activation. We propose to develop a more sophisticated approach, that we call time-frequency detection (TFD), to detect neural activation using knowledge of the EEG in the time-frequency plane. We illustrate this approach using an example from our pilot data.

Figure 4 shows time-frequency plots of EEG activity recorded over the visual cortex, during visual stimuli (left column) and at rest (right column). Each plot aligns the maximal negative peak to the zero point on the time-axis. Of main interest is the observation that the maximal negative peak (at zero) is consistently preceded by increased power and phase coherence. Referring back to Figure 1 we see that the left red circle in Figure 1A highlights a significant negative peak that is preceded by a power increase at 5-6 Hz, as shown by the left red arrow in Figure 1B. The right red circle in Figure 1A highlights the negative peak chosen by the BH-method, however this peak is *followed* by a 5-6 Hz power increase rather than being preceded by one. The peak in the left red circle of Figure 1A therefore has time-frequency characteristics that are more representative of the average task and rest time-frequency plots shown in Figure 4, and suggests that the red cross shown in Figure 1C may be the better activation point in the resting-state BOLD time-series. Our TFD method will use information from the time-frequency spectrum, as illustrated here, and from time-frequency coherence, to cluster significant negative peaks (that exceed a set threshold, e.g. 2 standard deviations). This could potentially create more than one distinct cluster, or alternatively generate one cluster with disparate outliers suggestive of artifact. Each cluster, if there is more than one, would then represent the time-locations of negative peaks that can then be used to either average the BOLD time-series (as in the BH-method) or deconvolve the BOLD time-series, using ordinary least squares, to estimate the hemodynamic response. Two or more clusters might be indicative of more than one process of neurovascular coupling, which might occur when only part of the local network is affected by disease.

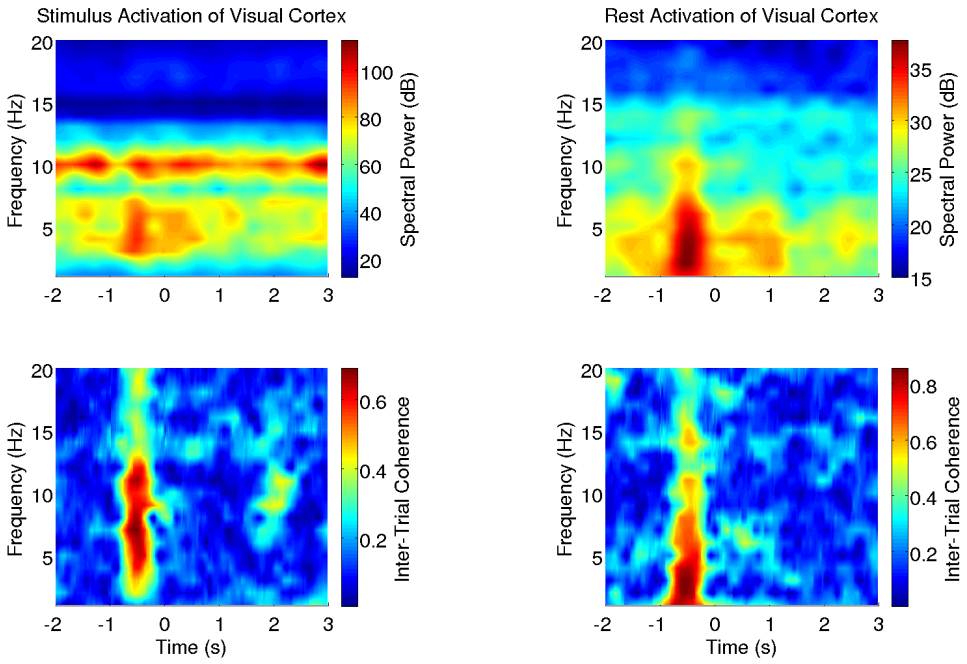

Figure 4 Time-frequency plots of EEG activity over the visual cortex, showing the frequency content at each time point. The left column shows average activity during visual stimuli. The right column shows average activity following detected negative peaks (using the BH-method – refer to text; Bruyns-Haylett et al 2013). The top row shows time-frequency plots of spectral power. The bottom row shows time-frequency plots of instantaneous phase, averaged across all detected peaks, and calculated as inter-trial coherence: a value between 0 (no phase coherence between trials) and 1 (perfect phase coherence between trials). The zero time-point is aligned with the maximal detected negative peak (see text). Of particular interest is that the maximal negative peak (zero time-point) is consistently preceded by increased power and increased coherence for both the visual stimulus and during rest. This was also observed at the motor cortex for both movement and rest (data not shown for brevity).

Specific Aim 2: Estimating the Hemodynamic Response throughout the Cortex

The TFD method to identify R-HRF could equally be applied to any location throughout the cortex. We will derive neural source estimates throughout the cortex using source localization software (Gramfort et al 2014). Source estimates will be constrained to the subject-specific cortical ribbon calculated from a T1 MRI image using Freesurfer software (Dale et al 1999). The TFD method will then be applied to each co-located source estimate and BOLD time-series to produce an R-HRF estimate at each cortical location. Each R-HRF will be fitted to a six parameter two-gamma-function model, which will quantify the peak and undershoot magnitude, peak and undershoot width, time-to-onset, and time-to-peak. Cortical maps will be created for each R-HRF parameter, which can then be used for statistical comparison or disease classification.

Specific Aim 3: Validating of the Time-Frequency Detection Method

We will perform a series of FMRI protocols to compare the E-HRF at different locations throughout the cortex with the R-HRF obtained by the TFD method. As event-related FMRI tasks require many repetitions to activate only a few cortical sites we will be limited to only a few sites for comparison. These will include the same method we used for our preliminary data to elicit hemodynamic responses in the primary visual and motor cortices, and similar methods to activate and measure the

hemodynamic response in auditory cortex and association cortices. We will pay particular attention to testing event-related FMRI tasks that activate areas of cortex in and near arterial border zones – i.e. cortical territories near the border between the anterior, middle, and posterior arteries. We will also use a breath-holding task to measure the relative timing difference between voxels (Chang et al 2008) and compare that with the relative timing of the time-to-peak and time-to-onset parameters that we estimate from the R-HRF.

Specific Aim 4: Characterizing the neurophysiological and hemodynamic processes in cortical vascular border zones and cortical association areas in a population sample

We will use the TCD method to characterize NVC in cortical areas that are vulnerable to pathology associated with Alzheimer's disease (AD).

Cortical vascular border zones are the first cortical areas to be deprived of sufficient blood flow in cerebral hypoperfusion, and are a prominent site of microinfarcts associated with AD (Suter et al 2002). Currently, microinfarcts are too small to be seen by current brain imaging methods (Smith et al 2012), yet they are known, from autopsy studies, to be prevalent in the sub-clinical population (Montine et al 2012). It is important, therefore, to develop methods that either detect microinfarcts directly or detect the conditions of hypoperfusion that support their genesis.

AD is also associated with reduced regional cerebral glucose metabolism in cortical association areas, with relative sparing of primary sensory and motor areas (Liang et al 2008; Minoshima et al 1995; Mielke et al 1994). In particular, metabolic changes in the posterior cingulate cortex (PCC) are observed in young, cognitively normal people at genetically greater risk of AD, prior to the onset of other observable AD pathology, such as amyloid plaques (Rieman et al 2005). Early detection of metabolic changes in PCC could, therefore, be predictive of prospective AD and prompt early pharmacologic intervention that could delay onset of the disease. This is significant because delaying the onset of AD by five years has the potential to reduce the economic cost of care by $50 billion over a five year period (www.alz.org/trajectory).

We will randomly select 50 subjects from the Adult Changes in Thought study (ACT) (Montine et al 2012) and invite them to participate in our neuroimaging study. This is a well characterized population-based sample of men and women over the age of 65, who are followed every two years with medical and cognitive evaluations until death or diagnosis with dementia. The ACT study has an autopsy endpoint, with a current level of 21% of those who have died having consented to autopsy.

From each subject we will acquire a structural MRI image, a fluid attenuated inversion recovery image (FLAIR), an arterial spin labeling (ASL) image, and a 10 minute resting-state scan of EEG simultaneously acquired with FMRI. Total MRI scan time will be 30 minutes. Twenty of these subjects will undergo 30 minutes of additional scan time to acquire event-related FMRI for the validation protocols described above. Thus, the project will require 30 hours of MRI scan time and 25 hours of EEG headcap setup time (30 minutes per subject).

We will use the FLAIR image to estimate the volume of white mater hyperintensities (WMH), which provides a surrogate marker for arteriolosclerosis (Erten-Lyons et al 2013), and are highly prevalent in people over the age of 65 (Launer 2004; Liao et al 1996). ASL will provide an estimate of cerebral perfusion as a surrogate for neural metabolism (Detre et al 2009).

A first analysis will use a general linear model (GLM) to measure the regional association between R-HRF parameters with cerebral perfusion across subjects. The GLM will also include each subjects' apolipoprotein E (APOE) epsilon-4 gene dose (i.e., the number of epsilon-4 alleles in a person's APOE genotype) as a separate factor, which is a known predictor of reduced metabolism in parietal and frontal association cortices (Rieman et al 2005). Age will also be entered as a covariate as it is another predictor of cerebral metabolism (Moeller et al 1996). We will test the following hypotheses:

1. R-HRF parameters will have age-adjusted predictive power of reduced metabolism over and above that of APOE epsilon-4 status.
2. The association between R-HRF parameters and cerebral metabolism will be strongest in locations of reduced cerebral perfusion.
3. APOE epsilon-4 gene dose will have a graded relationship with R-HRF parameters in the PCC and precuneus, due to the known effect of APOE status on metabolism in those regions (Rieman et al 2005).

A second analysis will use a GLM to measure the regional association between R-HRF parameters with WMH volume, and test the hypothesis that R-HRF parameters will have age-adjusted predictive power of WMH proximal to the WMH.

A third analysis will examine the relationship of R-HRF parameters with their proximity to cortical vascular border zones. Vascular border zones will be demarcated using masks of the anterior, middle, and posterior cerebral arteries, created from the atlas of Kretschmann and Weinrich (Mandell 2013; Kretschmann & Weinrich 2004). Within areas of cerebral vascular border zones we will use lines geometrically normal to each border zone and plot R-HR parameters along each line. We hypothesize that R-HR parameters will change as a function of distance from the border zone, and that these effects will be exacerbated in subjects with high WMH volume.

References

Alzheimer's Association. Changing the trajectory of Alzheimer's disease: A national imperative. www.alz.org/trajectory

Bruyns-Haylett M, Harris S, Boorman L, Zheng Y, Berwick J, Jones M. 2013. The resting-state neurovascular coupling relationship: rapid changes in spontaneous neural activity in the somatosensory cortex are associated with haemodynamic fluctuations that resemble stimulus-evoked haemodynamics. 2013. Eur J Neurosci, 38(6):2902-16

Chang C, Thomason ME, Glover GH. 2008. Mapping and correction of vascular hemodynamic latency in the BOLD signal, Neuroimage 43:90-102

Dale AM, Fischl B, Sereno MI, 1999. Cortical surface-based analysis. I. Segmentation and surface reconstruction. Neuroimage 9, 179-194.

Detre JA, Wang J, Wang Z, Rao H. 2009. Arterial spin-labeled perfusion MRI in basic and clinical neuroscience. Curr Opin Neurol, 22(4):348-55

Erten-Lyons D, Woltjer R, Kaye J, Mattek N, Dodge HH, Green S, Tran H, Howieson DB, Wild K, Silbert LC. 2013. Neuropathologic basis of white matter hyperintensity accumulation with advanced age. Neurology, 81(11):977-83

Girouard H, and Iadecola C. 2006. Neurovascular coupling in the normal brain and in hypertension, stroke, and Alzheimer disease. J Appl Physiol 100(1):328-35

Gramfort A, Luessi M, Larson E, Engemann D, Strohmeier D, Brodbeck C,Parkkonen L, Hämäläinen M, 2014. MNE software for processing MEG and EEG data, NeuroImage, 86:446-60

Iadecola C. 2004. Neurovascular regulation in the normal brain and in Alzheimer's disease. Nat Rev Neurosci, 5(5):347-60

Iannetti GD, Niazy RK, Wise RG, Jezzard P, Brooks JC, Zambreanu L, Vennart W, Matthews PM, Tracey I. 2005. Simultaneous recording of laser-evoked brain potentials and continuous, high-field functional magnetic resonance imaging in humans. NeuroImage, 28(3):708-19

Kretschmann, H., & Weinrich, W. (2004). Cranial neuroimaging and clinical neuroanatomy. New York: Georg Thieme Verlag.

Launer LJ. 2004. Epidemiology of white matter lesions. Top Magn Reson Imaging, 15(6):365-7

Liang WS, Reiman EM, Valla J, Dunckley T, Beach TG, Grover A, Niedzielko TL, Schneider LE, Mastroeni D, Caselli R, Kukull W, Morris JC, Hulette CM, Schmechel D, Rogers J, Stephan DA. 2008. Alzheimer's disease is associated with reduced expression of energy metabolism genes in posterior cingulate neurons. Proc Natl Acad Sci, 105(11):4441-6

Liao D, Cooper L, Cai J, Toole JF, Bryan NR, Hutchinson RG, Tyroler HA. 1996. Presence and Severity of Cerebral White Matter Lesions and Hypertension, Its Treatment, and its Control. The ARIC Study. Atherosclerosis Risk in Communities Study. Stroke, 27(12):2262-70

Mandell DM. 2013. Magnetic Resonance Mapping of Cerebrovascular Reserve: Steal Phenomena in Normal and Abnormal Brain. PhD thesis. Institute of Medical Science, University of Toronto.

Mielke R, Herholz K, Grond M, Kessler J, Heiss WD. 1994. Clinical deterioration in probable Alzheimer's disease correlates with progressive metabolic impairment of association areas. Dementia, 5(1):36-41

Miklossy J. 2003. Cerebral hypoperfusion induces cortical watershed microinfarcts which may further aggravate cognitive decline in Alzheimer’s disease. Neurol Res, 25(6):605-10

Minoshima S, Frey KA, Koeppe RA, Foster NL, Kuhl DE. 1995. A diagnostic approach in Alzheimer's disease using three-dimensional stereotactic surface projections of fluorine-18-FDG PET. J Nucl Med, 36(7):1238-48

Moeller JR, Ishikawa T, Dhawan V, Spetsieris P, Mandel F, Alexander GE, Grady C, Pietrini P, Eidelberg D. 1996. The metabolic topography of normal aging. J Cereb Blood Flow Metab, 16(3):385-98

Montine TJ, Sonnen JA, Montine KS, Crane PK, Larson EB. 2012. Adult Changes in Thought study: dementia is an individually varying convergent syndrome with prevalent clinically silent diseases that may be modified by some commonly used therapeutics. Curr Alzheimer Res, 9(6):718-23

Mullinger KJ, Mayhew SD, Bagshaw AP, Bowtell R, Francis ST. 2013. Poststimulus undershoots in cerebral blood flow and BOLD fMRI responses are modulated by poststimulus neuronal activity, Proc Natl Acad Sci, 110(33):13636-41

Niazy RK, Beckmann CF, Iannetti GD, Brady JM, Smith SM. 2005. Removal of FMRI environment artifacts from EEG data using optimal basis sets. NeuroImage, 28(3):720-37

Reiman EM, Chen K, Alexander GE, Caselli RJ, Bandy D, Osborne D, Saunders AM, Hardy J. 2005. Correlations between apolipoprotein E epsilon4 gene dose and brain-imaging measurements of regional hypometabolism. Proc Natl Acad Sci, 102(23):8299-302

Riehle A, Wirtssohn S, Grun S, Brochier T. 2013. Mapping the spatio-temporal structure of motor cortical LFP and spiking activities during reach-to-grasp movements, Front Neural Circuits, 7:48

Smith EE, Schneider JA, Wardlaw JM, Greenberg SM. 2012. Cerebral microinfarcts: the invisible lesions. Lancet Neurol, 11(3):272-82

Suter O, Sunthorn T, Kraftsik R, Straubel J, Darekar P, Khalili K, Miklossy J. 2002. Cerebral hypoperfusion generates cortical watershed microinfarcts in Alzheimer disease. Stroke, 33:1986-1992

Van Zijl PCM, Hua J, Hanzhang L. 2012. The BOLD post-stimulus undershoot, one of the most debated issues in fMRI, Neuroimage, 62(2):1092-102

Wesolowski R, Gowland PA, Francis ST. 2009. Double acquisition background suppressed (DABS) FAIR at 3T and 7T: Advantages for simultaneous BOLD and CBF Acquisition. Proc ISMRM. Available at http://cds.ismrm.org/protected/09MProceedings/files/01526.pdf

Zlokovic BV. 2011. Neurovascular pathways to neurodegeneration in Alzheimer's disease and other disorders. Nat Rev Neurosci, 12(2):723-38